

# Synchronization of a Nonlinear Oscillator: Processing the Cf Component of the Echo-Response Signal in the Cochlea of the Mustached Bat

Ian J. Russell,<sup>1,4</sup> Markus Drexler,<sup>2</sup> Elisabeth Foeller,<sup>3</sup> Marianne Vater,<sup>4</sup> and Manfred Kössl<sup>2</sup>

<sup>1</sup>School of Life Sciences, University of Sussex, Brighton, BN1 9QG United Kingdom, <sup>2</sup>Zoological Institute, University of Frankfurt, 60323 Frankfurt am Main, Germany, <sup>3</sup>Neurobiology Section, Division of Biology, University of California, San Diego, La Jolla, California 92093-0357, and <sup>4</sup>Institute of Biochemistry and Biology, University of Potsdam, 14471 Potsdam, Germany

Cochlear microphonic potential (CM) was recorded from the CF2 region and the sparsely innervated zone (the mustached bat's cochlea fovea) that is specialized for analyzing the Doppler-shifted echoes of the first-harmonic ( $\sim 61$  kHz) of the constant-frequency component of the echolocation call. Temporal analysis of the CM, which is tuned sharply to the 61 kHz cochlear resonance, revealed that at the resonance frequency, and within 1 msec of tone onset, CM is broadly tuned with linear magnitude level functions. CM measured during the ongoing tone and in the ringing after tone offset is 50 dB more sensitive, is sharply tuned, has compressive level functions, and the phase leads onset CM by 90°: an indication that cochlear responses are amplified during maximum basilar membrane velocity. For high-level tones above the resonance frequency, CM appears at tone onset and after tone offset. Measurements indicate that the two oscillators responsible for the cochlear resonance, presumably the basilar and tectorial membranes, move together in phase during the ongoing tone, thereby minimizing net shear between them and hair cell excitation. For tones within 2 kHz of the cochlear resonance the frequency of CM measured within 2 msec of tone onset is not that of the stimulus but is proportional to it. For tones just below the cochlear resonance region CM frequency is a constant amount below that of the stimulus depending on CM measurement delay from tone onset. The frequency responses of the CM recorded from the cochlear fovea can be accounted for through synchronization between the nonlinear oscillators responsible for the cochlear resonance and the stimulus tone.

**Key words:** mustached bat; cochlea; microphonic potential; frequency tuning; resonance; synchronization; basilar membrane; tectorial membrane; cochlear amplifier; compromise frequency

## Introduction

Sensory processing in the mammalian cochlea is accomplished through interaction between the basilar membrane (BM) and the tectorial membrane (TM) (Davis, 1965). This interaction is mediated through the electromotile outer hair cells (OHCs) (Brownell et al., 1985; Dallos, 1992) that amplify low-level signals and compress high-level signals to provide the remarkable sensitivity and dynamic range of the cochlea (Robles and Ruggero, 2001). The timing of OHC feedback, which provides the amplification, is the subject of models, speculation, and invasive experimentation (Geisler and Sang, 1995; Markin and Hudspeth, 1995; Nilsen and Russell, 1999). The specialized sparsely innervated (SI) region of the mustached bat's cochlea (Kössl and Vater, 1995) (Fig. 1A), the site of one of the most highly tuned and

resonant biological structures (Kössl and Russell, 1995; Russell and Kössl, 1999), provides a unique opportunity to use relatively noninvasive techniques to explore the timing and magnitude of cochlear amplification and to understand how the TM and BM interact to provide this remarkable tuning. The SI and adjacent constant-frequency (CF2) regions, which together constitute the mustached bat's cochlear fovea, are specialized for analyzing the Doppler-shifted echoes of the first-harmonic ( $\sim 61$  kHz) of the CF2 component of the bat's echolocation call that is used to measure target velocity and to detect the wing beats of insects (Neuweiler, 1990). Electrophysiological (Suga et al., 1975; Suga and Jen 1977; Kössl and Vater, 1990) and BM displacement measurements from the SI region of the mustached bat's cochlea (Kössl and Russell, 1995; Russell and Kössl, 1999) reveal that the  $Q_{10dB}$  (center frequency/bandwidth 10 dB from the tip of the bandpass filter) values of mechanical or neuronal tuning curves can reach 600 (Fig. 1B). A resonance of such quintessential sharpness takes many cycles to develop and decay, which has the effect of slowing down cochlear sensory processing. A characteristic we have exploited to take timed snapshots of the responses of the cochlea to tones at frequencies close to the cochlear resonance, thereby enabling us to separate and analyze the processing steps.

Mechanical measurements made from the BM in the SI zone,

Received May 23, 2003; revised July 8, 2003; accepted July 9, 2003.

This work was supported by the Volkswagen Foundation, the Deutsche Forschungsgemeinschaft, the Royal Society, and the Wellcome Trust. We thank Frank Coro and Emanuel Mora for providing the opportunity, stimulating environment, and discussion that facilitated these experiments and Andrei Lukashkin and Mikhail Bashtanov for stimulating discussion and helpful criticism of early drafts of this manuscript.

Correspondence should be addressed to Prof. I. J. Russell, School of Biological Sciences, University of Sussex, Falmer, Brighton, BN1 9QG UK. E-mail: I.J.Russell@sussex.ac.uk.

Copyright © 2003 Society for Neuroscience 0270-6474/03/239508-11\$15.00/0

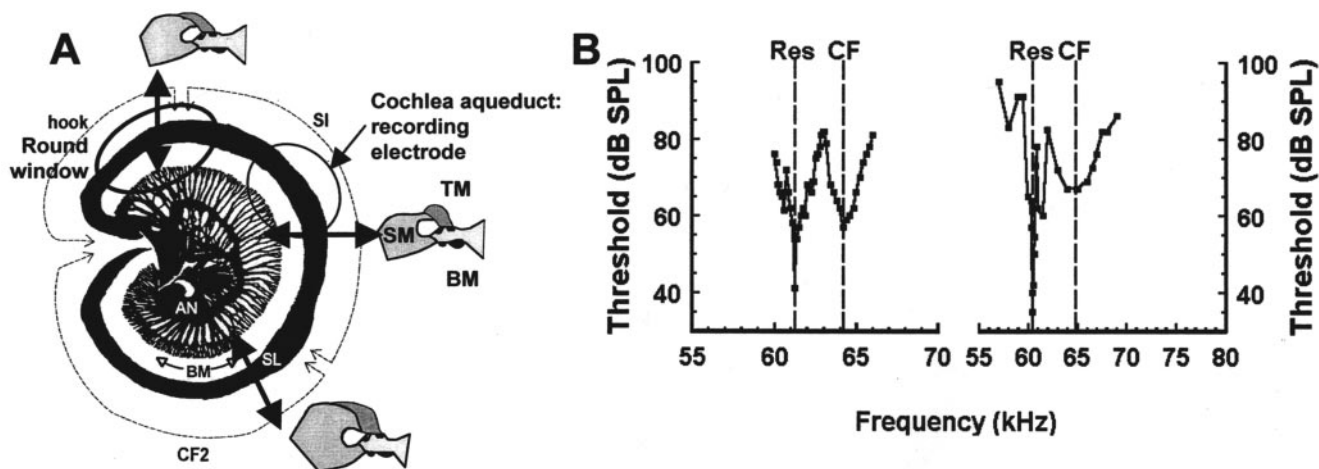


**Figure 1.** *A*, Cochlear anatomy in the mustached bat. Camera lucida drawing of whole mount of the basal turn with round window, BM, afferent nerve fibers (AN), and spiral ligament (SL). Two densely innervated regions (hook, CF2) are separated by the SI zone. At the transition between the SI and CF2 regions, the spiral ligament (SL) is enlarged. Cross sections of the organ of Corti are shown, where it can be seen that the attachment of the TM to the spiral limbus (SM) is greatly reduced and the BM is thickened in the SI region. *B*, Isoresponse basilar membrane tuning curve measured from the SI region of the mustached bat cochlea showing peaks at the cochlear resonance (Res) and the characteristic frequency (CF) (from Russell and Kössl, 1999).

reveals the BM to be tuned to both its characteristic frequency (62–72 kHz), in accordance with the cochlear frequency place map evident from labeling afferent dendrites (Kössl and Vater, 1985), and to the resonance frequency (61–62 kHz) (Fig. 1*B*). This is because the BM in the SI region supports both a traveling wave, which determines the place-sensitive tuning of the BM, and a standing wave that determines the cochlear resonance (Kössl and Russell, 1995; Russell and Kössl, 1999).

OHCs of the fovea constitute 40% of the total population of the cochlea and OHC responses to the 61 kHz signal dominate the cochlear microphonic potential (CM) recorded from the fovea. From CM measurements made from the fovea we describe the timing of presumed OHC feedback and its contribution to the amplification of tone-induced vibrations of the cochlear partition. We also obtain evidence of the OHC-mediated interaction between the TM and the BM that is the basis of the remarkable frequency tuning of the foveal region of the mustached bat's cochlea.

## Materials and Methods

Seven adult mustached bats were used in the present study. In four cases, the bats were brought to a laboratory in Havana and kept 1–3 d before the measurement of cochlear potentials. To measure CM and the compound action potential the bats were anesthetized with a Rompun and Ketavet mixture (Ketamine HCl 5 mg/ml, 2% Rompun, in the proportion 9:1; dose, 0.025–0.04 ml per 10 gm). In three cases, measurements were made from bats in a colony maintained in Germany, and the animals were maintained under gaseous isoflurane anesthesia. The skulls of the bats were fixed by dental acrylic to a metal bar and an insulated tungsten electrode was introduced through the cerebellum into the cochlear aqueduct for the purpose of recording the CM (Fig. 1*A*) (Henson and Pollak, 1972; Henson et al., 1985). The CM is a compound receptor potential that is largely, if not entirely, attributable to the responses of the OHCs (Dallos et al., 1972; Russell and Sellick, 1983; Dallos, 1985; Patuzzi et al., 1989). CM generated in the foveal region dominates recordings from the cochlear aqueduct.

While advancing the electrode toward the cochlear aqueduct, sound stimuli were presented and CM responses were measured. Typically, after reaching the aqueduct there was a sudden increase in CM magnitude that did not change substantially when the electrode was advanced further. Having reached this position we usually stopped the penetration and started the data acquisition. During the recordings the body temper-

ature was maintained with an infrared lamp. All experimental animals were anesthetized and they were killed with an overdose of the anesthetic at the end of the experiment.

Pure-tone sound stimuli of 10 msec duration with 1 msec cosine rise and fall envelopes were used for acoustic stimulation. The stimuli were generated by a Microstar (Bellevue, WA) 3000a/212 or a Microstar 4200a data acquisition board and subsequently attenuated by a computer-controlled attenuator (custom made by Jim Hartley, University of Sussex, Sussex, United Kingdom). Either MicroTech (Mühlberg, Germany) Gefell 1 inch MK102.1 inch microphone capsules or Polaroid type 6500 sonar speaker modules were used to generate sound stimuli. Constant sound pressure levels (SPLs) for different frequencies were guaranteed either by the use of online calculation of loudspeaker calibration curves or the SPLs were calculated offline from the calibration curves. For each data acquisition, 20–80 averages were used. The responses were fed into the Microstar board and programs written using Testpoint (Capital Equipment Corporation, Billerica, MA) were used to control data acquisition. In some cases the application of loud tones above 80 dB SPL caused attenuation of the response magnitude with a latency of 6–7 msec, which is typical for the effects of the middle ear muscle reflex (Suga et al., 1974; Henson et al., 1995). Data showing these characteristics were rejected.

The animal use in this study was authorized by the Centre for the Inspection and Control of the Environment, Ministry of Science, Technology and Environment, Cuba. The experiments comply with the "Principles of Animal Care," publication 86–23, revised 1985 of the National Institute of Health, with the Declaration of Helsinki, and also with German federal regulations (approved by the Regierung von Oberbayern, 211–2531–37/98).

## Results

### Sound-evoked electrical potentials from cochlear duct

The electrical signal recorded from the cochlear duct in *Pteronotus parnellii* in response to a tone burst consists of the CM, the compound action potential (CAP) of the auditory nerve and a brainstem field potential (FP) (Fig. 2). Typically the CM continues to ring for several milliseconds immediately after the offset of tones at or close to the ~61 kHz resonance frequency (Fig. 2, CM<sub>AFT</sub>), but not at frequencies >2 kHz above and below the resonance (Fig. 2, 63.4 kHz).

The ringing of a highly resonant structure, e.g., a tuning fork, takes time to build up and to decay. This time increases with the

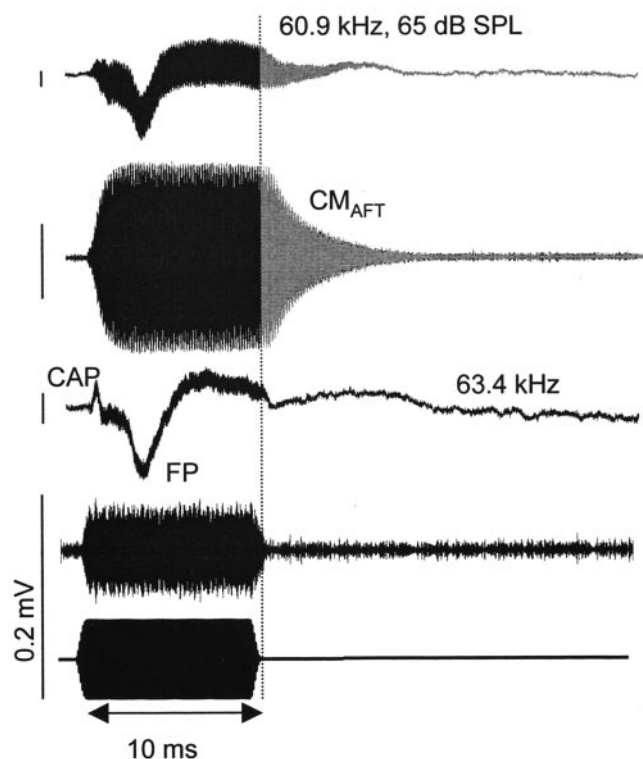


**Figure 2.** Electrical responses recorded from the cochlear ducts of a greater mustached bat with a cochlear resonance of 60.9 kHz in response to 10 msec tones (bottom record). Top two records, CM to a resonance frequency tone. Note ringing indicated by gray shading. Bottom two records, CM to a frequency above the resonance frequency. Note the absence of prolonged ringing. In each pair of records the top trace is high-pass-filtered at 50 Hz and the lower has been bandpass-filtered from 40 to 80 kHz.  $CM_{AFT}$ , Resonance. Vertical scales, 0.2 mV. Each trace is the average of 40 recordings.

sharpness of the resonance. The  $Q_{3dB}$  of the SI region of the cochlea can be very high ( $\sim 900$ ; Kössl and Russell, 1995), so that the CM in response to resonance frequency tones takes several milliseconds to build up and decay (Fig. 2). Thus, in a highly resonant system there is a trade-off between the frequency and temporal domains; frequency acuity is gained at the expense of temporal acuity. Accordingly, the sharp resonance of the cochlear foveal region results in a slowing down of sensory processing by the cochlea that provides an opportunity to explore temporal changes in the response properties and the frequency tuning. In this paper we measured CM within the first 1–2 msec of tone onset, during the ongoing tone, which we defined as 4–9 msec after tone onset, and during the ringing in the CM responses that follows tone offset, which we defined as  $>0.5$  msec from tone offset. CM measurements made during the first 1 msec of the tone are made during the rise time of the tone envelope that was used in these experiments to suppress stimulus onset transients. These dynamic stimulus conditions have been taken into account when calculating the magnitude of the CM during tone onset.

#### Magnitude–level functions at and close to resonance frequency become amplified and compressed over time

The magnitude of the CM as a function of sound level, which was measured for tones at frequencies within 5 kHz of the resonance frequency, is shown in Figure 3. The magnitude functions are constructed from 8192 point fast Fourier transforms (FFTs) that were applied to data that were sampled for 1 msec periods beginning at 0.8 (onset), 8 (ongoing), and 15 (offset ringing) msec

from the onset of 10 msec duration tones. The data were sampled at 4  $\mu$ sec intervals. Thus, the data points filled only  $\frac{1}{32}$  of the 8192 FFT array and the remainder of the array was filled with the final value of the data trace. This process was carried out in every case in which the number of data points did not match the size of the FFT array. Data analyzed in this way provided an  $\sim 30$  Hz resolution for measurements of the magnitude and phase of CM responses.

Magnitude–level functions that were measured at 59.0, 61.0, and 62.3 kHz from the cochlea of a bat with a cochlear resonance of 61.0 kHz are shown in Figures 3A–C, 7G, and 9C. For tones more than  $\sim 0.5$  kHz above and below the resonance frequency (Fig. 3A,C), the CM is relatively insensitive and grows linearly with increasing SPL. There is no measurable CM response 5 msec after the offset of 59.0 kHz tones, and the onset and offset CM in response to 62.3 kHz tones are similar in magnitude and level dependency. At, and very close to, resonance frequency (Fig. 3B), the level functions measured during the steady-state (8 msec from tone onset) and in the ringing after tone offset (measured 5 msec after tone offset) are very similar, being saturating and  $\sim 50$  dB more sensitive than the linear, noncompressive level function obtained at tone onset. Thus, within 1 msec of the onset of a resonance-frequency tone, the mustached bat cochlea behaves as a mechanically passive structure. Amplification of responses in the mustached bat's cochlea takes several milliseconds to develop.

#### With increasing time from tone onset, the resonance peak of the magnitude–frequency function is amplified, sharpened, and shifted upward in frequency

CM magnitudes as functions of tone frequency measured at a constant level for 10 msec duration tones within 3 kHz of the resonance frequencies, at different times from tone onset, are shown together with examples of the raw data from which they are derived for three different preparations, in Figures 4 and 5. The data are based on FFTs applied to 1 msec data windows that are collected with increasing delays from tone onset. After tone onset, the delays are incremented in 0.1 msec intervals for the first millisecond, 0.2 msec intervals for the next millisecond, and thereafter in 1 msec intervals over a range of frequencies from 58 to 64 kHz (see figure captions). In all cases (Fig. 4C,D) the frequency magnitude curves are broad and insensitive when measured early in the tone burst. The curves become narrower and increase in magnitude, particularly at the peak as the data collection window is shifted later into the period of the tone burst. The data in Figure 4A,B show the characteristic beating between the response to the stimulus tone and the resonance. The resonance frequency can be determined as that frequency when beating is absent (A, 61.0 kHz; B, 62.4 kHz). The resonance frequency can also be obtained from the beating interval, which increases when the stimulus frequency approaches that of the cochlear resonance. The interval extends to infinity at the resonance frequency and decreases again when the cochlear resonance frequency is exceeded. The relationship between the beat interval and stimulus frequency, which is plotted in Figure 4E for a cochlea with a resonance at 61.4 kHz and for the data shown in Figure 4B (resonance, 62.4 kHz), provides a description of the tuning characteristics of the cochlear resonance. The frequency of the cochlear resonance can also be obtained by adding the beat frequency to the stimulus frequency for frequencies that are less than the cochlear resonance frequency and subtracting the beat frequency from the stimulus frequency for frequencies that are more than cochlear resonance (Fig. 4F).



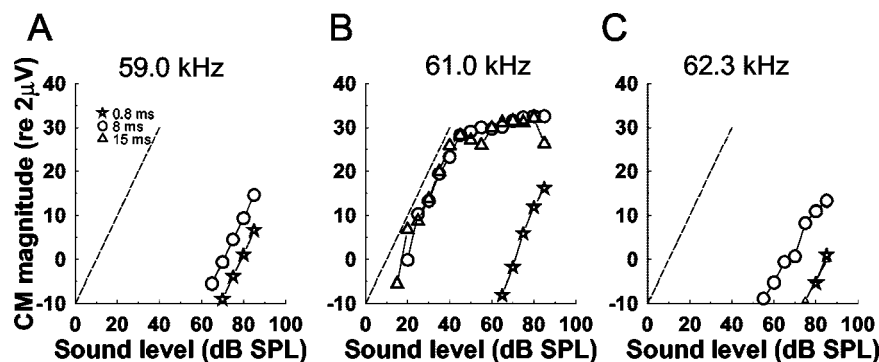


**Figure 3.** CM magnitude as a function of level measured from a bat with a cochlear resonance at 61.0 kHz in response to 10 msec duration tones at frequencies just below (*A*), at (*B*), and just above (*C*) the cochlear resonance, as functions of level measured 0.8 (asterisks), 8 (circles), and 15 msec (triangles) from tone onset. Ordinates are measured in decibels with respect to 2  $\mu$ V and the dotted line represents linear growth rate.

The curves in Figure 4C are based on CMs measured from a cochlea with a prolonged ringing and sharply tuned resonance ( $Q_{3dB} = 265$ ) and a CM gain at the resonance frequency from tone onset to a maximum of  $>60$  dB (Fig. 4C). The curves show considerable frequency-dependent microstructure that is preserved over time. In contrast the magnitude level functions in Figure 4D, which are based on CM recorded from a cochlea with a brief ringing, a relatively broadly tuned ( $Q_{3dB} = 113$ ) resonance, and CM gain at the resonance frequency from tone onset to maximum of  $>30$  dB, develop smoothly over time without significant microstructure.

CM recorded from one bat that was anesthetized with isoflurane displayed characteristic beating between the resonance and the stimulus tone for frequencies close to the resonance. However, the CM recordings were remarkable in that additional beating was present during  $CM_{Steady}$  and  $CM_{AFT}$ , that was unrelated to the frequency of the stimulus tone (Fig. 5A). In other words, the resonance of this bat was attributable to the interaction of two oscillators that were close in frequency. From the beating periodicity measured in  $CM_{AFT}$  it is apparent that the natural frequency of one oscillator is at the cochlear resonance frequency of 61.97 kHz and the other is 62.18 kHz (Fig. 5B). The magnitude–frequency functions (Fig. 5C) have complex microstructures that are preserved over time from tone onset, particularly for frequencies  $<60$  kHz and  $>61$  kHz and the  $Q_{3dB}$  of the resonance = 156. The peak of the magnitude–frequency functions appears in fact to be a double peak (61.9 and 62.1 kHz) separated by a notch at 62.0 kHz.

### CM phase

CM phases as functions of tone frequency at different tone levels is plotted from measurements made from four sensitive bats at different sound levels in the upper parts of Figures 6. The corresponding magnitude is plotted in the lower parts of these figures. Phase and magnitude were measured within 1.0 msec of tone onset (squares,  $CM_{ON}$ ), during the ongoing tone (4–9 msec from tone onset; circles,  $CM_{Steady}$ ), and 0.5–1.5 msec after tone offset (triangles,  $CM_{AFT}$ ) as indicated by the shaded areas of records in Figure 7A. A longer measurement period was used during  $CM_{Steady}$  to average out phase jitter (see below). Phase differences ( $CM_{Steady} - CM_{ON}$ , thin line;  $CM_{AFT} - CM_{ON}$ , thick line) are shown in the top part of the figure. Phase measurements for all four bats are similar.

### Phase–frequency relations of $CM_{ON}$

For frequencies within 5 kHz below the cochlear resonance, the slope of the  $CM_{ON}$  phase–frequency relationship is 1.8–2.0 radians/kHz. For frequencies within 200–400 Hz of the resonance frequency,  $CM_{ON}$  phase either becomes constant and frequency-independent (Fig. 6A,B), or converts to a phase lead (Fig. 6C,D). For frequencies above resonance,  $CM_{ON}$  returns to a phase lag with increasing frequency.

### $CM_{Steady}$ phase leads $CM_{ON}$ below resonance

CM phase as functions of tone frequency for  $CM_{Steady}$  lead that of  $CM_{ON}$  for frequencies below the resonance. The slope of  $CM_{Steady}$  is similar to that of  $CM_{ON}$  (1.8–2.0 radians/kHz), but decreases to  $\sim 1$  radian/kHz within 1 kHz of the CF. Consequently,  $CM_{Steady}$  phase leads  $CM_{ON}$  by  $\sim 90^\circ$  for frequencies that are  $<1$  kHz below the resonance. Within 100–300 Hz of the resonance, the slope of  $CM_{Steady}$  phase versus frequency increases and the  $CM_{ON}$  and  $CM_{Steady}$  phase–frequency functions intersect at the resonance.  $CM_{ON}$  and  $CM_{Steady}$  are in phase for tone frequencies above the resonance.

### $CM_{AFT}$ phase leads then lags $CM_{ON}$ below and above resonance

The phase of  $CM_{AFT}$  leads  $CM_{Steady}$  for frequencies below the resonance (Figs. 6 and 7). Within 1 kHz of the resonance, the slope of the  $CM_{AFT}$  phase–stimulus frequency relationship is 4–5 radians/kHz, which is twice as steep as those of  $CM_{ON}$  and  $CM_{Steady}$ . This greater slope of the  $CM_{AFT}$  phase–stimulus frequency relationship is because the  $CM_{AFT}$  has a single frequency component, which is that of the cochlear resonance; this changes in phase with respect to the stimulus frequency when the stimulus frequency is changed. Thus,  $CM_{AFT}$  leads  $CM_{ON}$  by  $\sim 360^\circ$  at a frequency 1 kHz below the resonance, which declines to a lead of  $180^\circ$  100 Hz below the resonance. The slope of  $CM_{AFT}$  phase–stimulus frequency relationship is very steep through the resonance, and it intersects the phase–stimulus frequency relationships of  $CM_{ON}$  and  $CM_{Steady}$ . For frequencies above the resonance,  $CM_{AFT}$  lags  $CM_{ON}$  and  $CM_{Steady}$  by  $180^\circ$ .

### CM on–off responses attributable to interaction between two oscillators

The CM on–off response is a phenomenon in which the CM appears transiently at tone onset and as a ringing that starts during the envelope of the tone at the offset, but is canceled during the ongoing-tone burst (Fig. 7A, 62 kHz). As a general rule, the CM on–off response is elicited by tones at levels  $>75$  dB SPL and at frequencies 0.5–2 kHz above and below the resonance frequency, but the conditions are specific to the particular cochlea from which the measurements are made. Thus, the CM on–off response is clearly visible in Figure 7A, which was obtained at 90 dB SPL, but not in the data of Figures 4–6, in which the levels did not exceed 75 dB SPL. Although Suga et al. (1975) specifically referred to this form of response as *CM-off*, there is also a pronounced peak in the CM at tone onset and the magnitude of the CM during the ongoing tone (Fig. 7A, 62 kHz) can be disappearingly small. In an attempt to understand the basis for CM on–off responses, magnitude and phase as functions of tone frequency

were measured for  $CM_{ON}$  (squares),  $CM_{Steady}$  (circles), and  $CM_{AFT}$  (triangles), as indicated by the stippled regions in Figure 7A. The curves are shown in Figure 7B. The phase relationships of the CM measured during  $CM_{Steady}$  and  $CM_{ON}$  and  $CM_{AFT}$  are similar to those shown in Figure 6, and the frequency–phase relations of  $CM_{Steady}$  and  $CM_{ON}$  and  $CM_{AFT}$  all intersect at the resonance (61 kHz), although at 90 dB SPL and from 60.5 to 62.5 kHz the  $CM_{ON}$  phase does not change. There is a sharp minimum in the  $CM_{Steady}$  magnitude–frequency curve at 61.9 kHz (marked with a vertical dashed line). At this frequency,  $CM_{AFT}$  leads  $CM_{ON}$  by almost exactly one cycle and is in phase with  $CM_{ON}$  (Fig. 7B). At this frequency the  $CM_{ON}$  phase lags  $CM_{Steady}$  by  $90^\circ$  and the  $CM_{AFT}$  phase leads  $CM_{Steady}$  by  $270^\circ$ . Accordingly, at this particular combination of stimulus frequency and level OHCs are excited during tone onset and at and after tone offset, when there is a phase difference between  $CM_{ON}$  and  $CM_{AFT}$ , but not during the ongoing tone, when the phase difference between  $CM_{ON}$  and  $CM_{AFT}$  is at or very close to zero. Level functions shown in Figure 7C for  $CM_{Steady}$  and  $CM_{ON}$  and  $CM_{AFT}$  measured at 61.9 kHz reveal a phase cancellation notch at 90 dB SPL in  $CM_{Steady}$ , but not in  $CM_{ON}$  and  $CM_{AFT}$ .

OHCs are not excited when the oscillators that drive  $CM_{ON}$  and  $CM_{AFT}$  move together in phase. This conclusion is supported by the analysis of the frequency composition of  $CM_{ON}$ ,  $CM_{Steady}$ , and  $CM_{AFT}$  (Fig. 8). If we select dominant peaks in the FFT that are  $<15$  dB above the measurement noise floor, then  $CM_{ON}$  is dominated by the natural frequency of the onset oscillator, which is 60.854 kHz, and also a higher frequency mode at 64.146 kHz (Fig. 8A).  $CM_{Steady}$  (Fig. 8B,C) contains a component at the stimulus frequency (61.83 kHz) and the higher frequency mode of the onset oscillator (64.146 kHz).  $CM_{AFT}$  contains only a single frequency component at 61.098 kHz, which is attributable to the offset oscillator that has a natural frequency 0.2 kHz higher than that of the onset oscillator.

#### CM frequency at tone onset for near-resonance frequency tones is not that of tone and has several modes

To investigate temporal changes in CM responses to 10 msec tones for frequencies near the resonance, we measured the frequency of the CM at 0.1 msec intervals during the first 3 msec of the tone and then at 1 msec intervals during the remainder of the tone and for a period of up to 9 msec after the cessation of the tone. Depending on the preparation, these measurements were made for a series of tones stepped either in 0.1 or 0.2 kHz increments from 2 to 5 kHz above and below the resonance frequency.

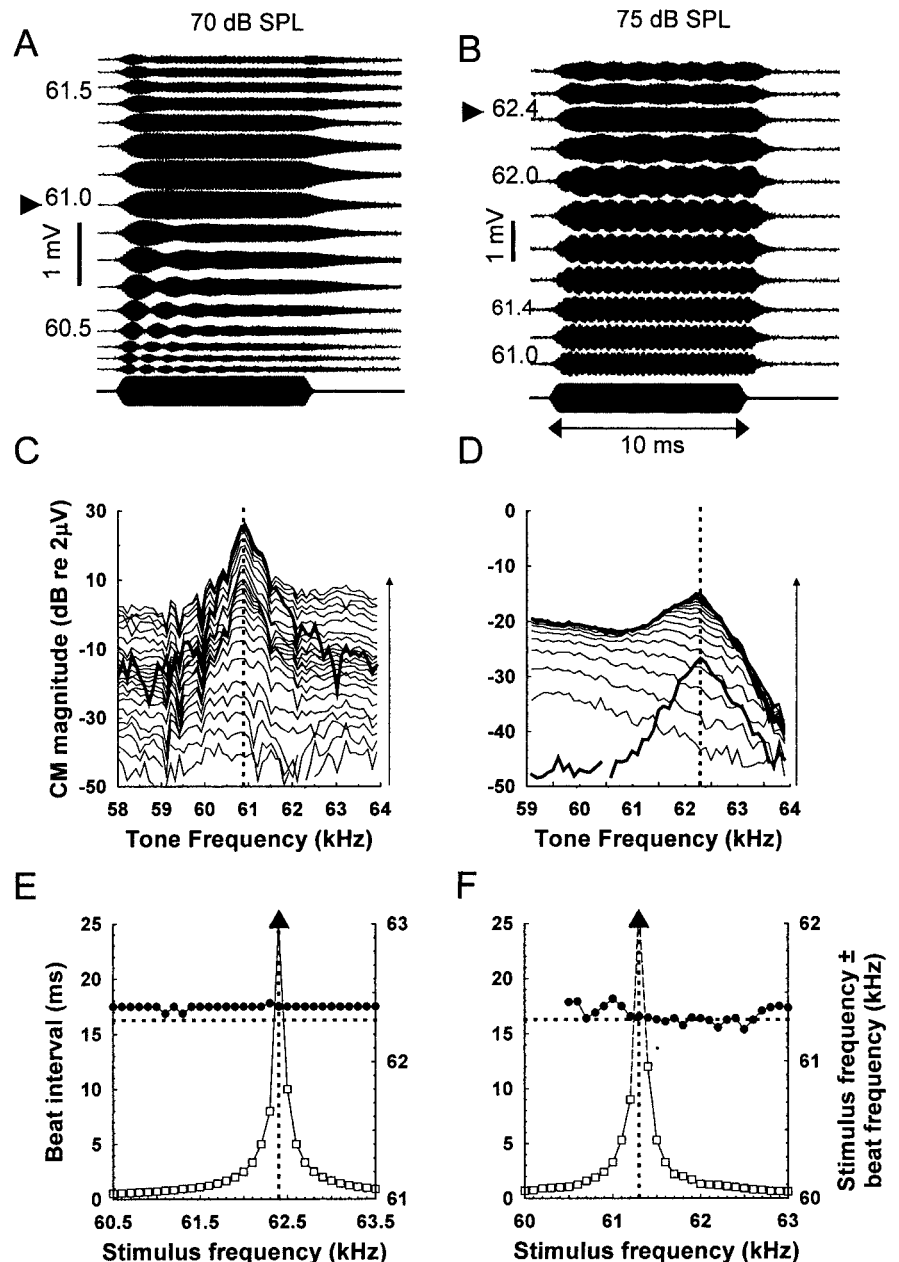


**Figure 4.** With increasing time from tone onset, the resonance peak is amplified, sharpened, and shifted upward in frequency. *A, B*, CM (filtered, 40–80 kHz) recorded from the cochlear duct (arrows indicate resonance: *A*, 61 kHz; *B*, 62.4 kHz) in response to 10 msec tones (bottom). *C, D*, CM magnitude as a function of stimulus frequency measured with delays from tone onset of 0.6–10.0 msec. Direction of increasing delay indicated by long arrow on right. Thick line,  $CM_{AFT}$  (11.5–12.5 msec); dotted line, resonance frequency. *E, F*, The modulation (beat) interval of the  $CM_{Steady}$  shown in *A* and *B* as a function of stimulus frequency (squares), which tends to infinity at the resonance frequency, and the stimulus frequency  $\pm$  the beat frequency as a function of stimulus frequency (circles), which gives the resonance frequency.

The frequency and magnitude of the CM was determined from 8192 point FFTs (see above for method) applied to 1 msec sample periods of the CM.

#### CM at tone onset produced by system with several frequency modes

CM measurements in response to 70 dB SPL tones centered on the resonance frequency are shown in Figure 4A for a sensitive bat with sustained ringing at tone offset. These data, expressed as the frequency of the maximum frequency component of the CM as a function of time, are shown in Figure 9A, and CM frequency

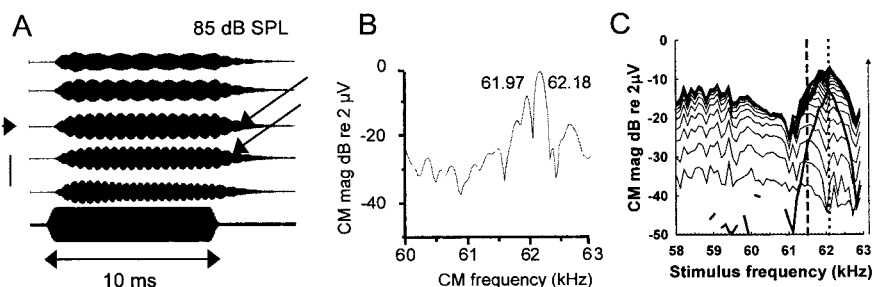


**Figure 5.** Responses from a cochlea with mismatched oscillators. *A*, CM (bandpass-filtered, 20–80 kHz; mean of 40 averages; vertical bar, 0.1 mV) in response to tones 100 and 200 Hz above and below the 62.1 kHz resonance (arrowhead). Beating occurs between the resonance and stimulus frequency and between two intrinsic oscillators during the tone and in ringing after tone offset (arrows). *B*, FFT (4096 points, 4  $\mu$ sec interval) applied to ringing after the 62.1 kHz tone shown in *A* reveals the frequencies of the two beating oscillators (61.97 and 62.18 kHz) whose frequency difference would account for the beating in ringing. *C*, CM magnitude as a function of stimulus frequency measured with 0.5–10.0 msec delays from tone onset. Direction of increasing delay indicated by long arrow on right. Broadly tuned, low-frequency oscillator (peak indicated by dashed line) appears  $<0.5$  msec from tone onset. Responses from the sharply tuned oscillator (peak indicated by dotted line) appear 0.6 msec from tone onset. The peak of this curve is separated from the lower-frequency peak by a notch at 62 kHz. Thick curve,  $CM_{AFT}$  (11.5–12.5 msec).

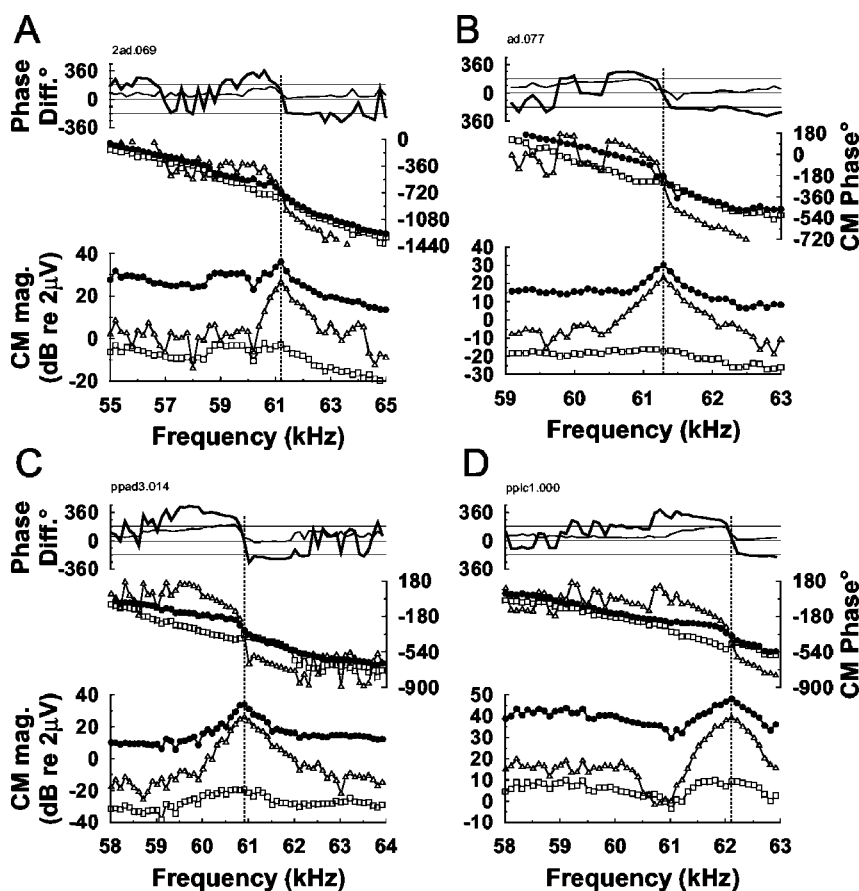


**Figure 6.** CM magnitude (bottom), CM phase (middle), and CM phase difference (top) as functions of tone frequency measured in four different bats at the frequencies shown and at the following levels: *A*, 70; *B*, 65; *C*, 55; and *D*, 60 dB SPL. Squares,  $CM_{ON}$  measured 0–1 msec from tone onset; circles,  $CM_{steady}$  measured 4–9 msec from tone onset; triangles,  $CM_{AFT}$  measured 0.5–1.5 msec after tone offset. Top, thin line,  $CM_{steady} - CM_{ON}$ ; thick line,  $CM_{AFT} - CM_{ON}$ ; vertical dotted lines, resonance frequency. Measurements based on 8192 point FFTs applied to CM data.

and magnitude as functions of stimulus frequency are shown in Figure 9E. The FFTs upon which the data in Figure 9E are based are shown Figure 9B–D. For tones within the range of stimulus parameters shown in Figure 9A–E (70 dB SPL and 58–64 kHz), the onset CM frequency does not increase smoothly in proportion to the stimulus frequency, but as a series of sharp frequency

transitions separated by sloping steps (Fig. 9E). The frequency steps at 59.4 and 62.4 kHz are both close to 2 kHz in magnitude. We refer to the region between the two transition frequencies (indicated by vertical dotted lines) as the cochlear resonance region (CRR, see below).

The frequency of the CM is rarely that of the tone. It can be seen by the irregular traces in Figure 9A that within 3 to 10 msec of tone onset, the frequency of the tone oscillates irregularly about the stimulus frequency. After tone offset, the cochlea rings for many milliseconds at a single frequency (61.005 kHz). The frequency of the CM in the ringing is higher than that of the CM measured at tone onset, which is 60.8 kHz when driven by a 61 kHz tone (Fig. 9E). Within the CRR, the CM below the resonance is a compromise between the stimulus frequency and the resonance frequency for frequencies between 59.4 and 61 kHz (the resonance) (Fig. 9E). For frequencies above 61 kHz and the upper boundary of the CRR, the CM frequency is at, or very close to, the resonance, which indicates that the CM frequency is attracted to the resonance. This can be seen in Figure 9C,D, in which for frequencies between 61 and 62.7 kHz, FFTs peak either at the resonance frequency or have a complex peak with a lobe that is at, or attracted to, the resonance frequency. FFTs for CM responses to tones below the resonance have simple peaks that are not attracted to the resonance until they are very close to it (Fig. 9B,D).

#### Within ongoing tone, resonance component of CM suppressed by stimulus response for frequencies above resonance

The ongoing tone elicits a CM response to the stimulus tone (Fig. 9F, thin line) and a smaller response to the resonance (thick line) for frequencies below the resonance frequency (Fig. 9F, vertical dashed line, and inset of FFT in response to 60 kHz tone). For frequencies within 400 Hz of 60.9 kHz, the stimulus frequency attracts 61 kHz (which is the resonance) to 60.9 kHz, as can be seen in the dip of the thick trace in Figure 9F, top, compared with the thick dotted trace, which is the frequency of the ringing after tone offset as a function of the stimulus frequency. This shift in frequency is also apparent in the FFTs shown in the inset, in which the resonance peaks at 61 kHz in response to a 60 kHz tone but peaks at 60.9 kHz in response to a 61 kHz tone, as indicated by the arrow in the inset. For stimulus frequencies above the resonance frequency, the CM response to the resonance is suppressed by the CM response to the stimulus tone (Fig. 9F, thick line, and inset of FFT to 62 kHz tone).



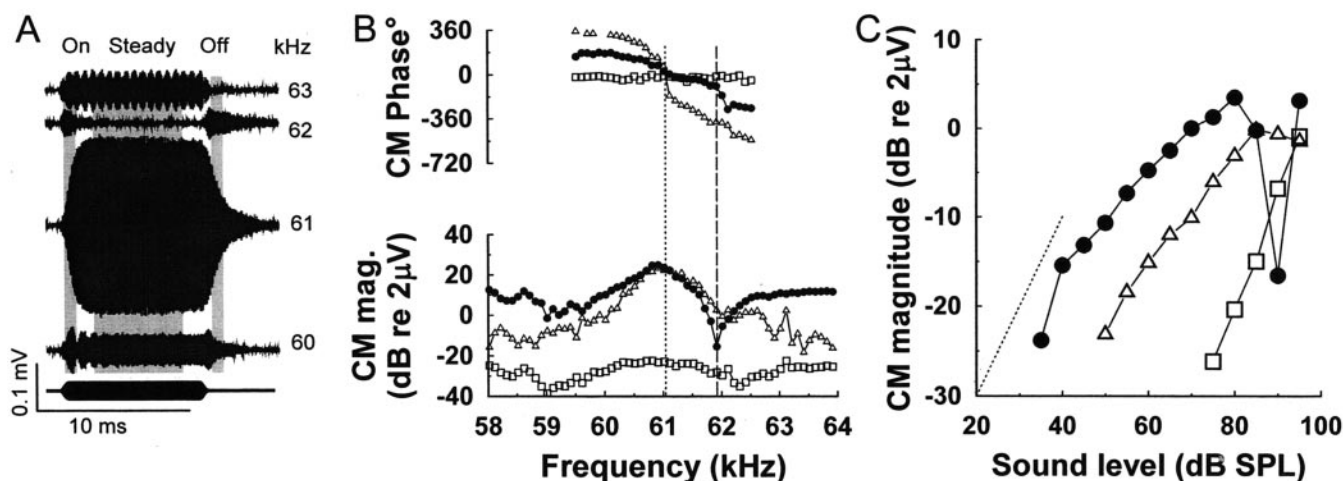


**Figure 7.** *A*, CM responses to tones at 60–63 kHz and 90 dB SPL. Note amplitude modulation as a consequence of beating between the stimulus frequency and the cochlear resonance in responses at 60 and 63 kHz. Note the strong cancellation of the CM during the 62 kHz tone and the residual CM responses during the dynamic phases of the onset and offset of the tone burst and during the ringing after tone offset. Stippled areas indicate measurement times at 0.6–1.6, 4–9, and 11–12 msec from the beginning of the tone burst. *B*, CM magnitude (bottom) and CM phase (top), as functions of frequency. Squares,  $CM_{ON}$  measured 0–0.7 msec from tone onset; circles,  $CM_{steady}$  measured 8–9 msec from tone onset; triangles,  $CM_{AFT}$  measured 0.5–1.5 msec after tone offset; vertical dotted line, resonance frequency; dashed line, minimum in steady-state magnitude. CM level functions measured in response to tones at 61.9 kHz at tone onset (squares), steady-state (circles), tone offset (triangles). Note cancellation notch at 90 dB SPL in steady-state CM. Dotted line, Slope of 1.

### Growth functions

Stimulus-evoked CM responses for frequencies below the resonance, measured during the ongoing tone, increase linearly with level for levels below saturation of the response (Fig. 9G, 75 dB SPL, 60 kHz).

The resonance-evoked CM response, whether measured in response to resonance frequency tones, or at frequencies below this, have steep slopes close to 1 (0.85). Tone-evoked CM response measured for frequencies above the resonance are very compressive, with slopes close to 0.5 (Figs. 7C and 9G).

### CM frequency at tone onset lower than that of stimulus tone at frequencies below CRR

The frequency difference between the CM and the tone as functions of tone frequency is plotted in Figure 10A. For measurements of CM within 2 msec of tone onset and for tone frequencies below the transition frequency (59.2 kHz) of the CRR, the slopes of the CM frequency functions parallel that of the isofrequency curve (Fig. 9B, vertical dashed line) but differ by a fixed amount that depends on the measurement delay from tone onset (e.g., 0.2 kHz for measurements made 1 msec after tone onset, 0.55 kHz for tones made 0.6 msec after tone onset).

### Synchronization as basis for CM frequency recorded from cochlear fovea at frequencies below CRR

The frequency behavior of the CM recorded from the cochlear fovea is exhibited by coupled oscillator systems, in which the oscillators do not run at their natural frequencies (e.g.,  $\omega_1$  and  $\omega_2$ ) but at a compromise frequency ( $\omega^*$ ) that is between the two and depends on the coupling strengths  $K_1$  and  $K_2$  of the two oscillators:

$$\omega_2 \xrightarrow{\Delta\omega_2} \omega^* \xleftarrow{\Delta\omega_1} \omega_1$$

The relationship is given by:

$$\omega^* = (K_{1,\omega_2} + K_{2,\omega_1}) / (K_1 + K_2) \quad (1)$$

(Strogatz, 1994), where

$$|\omega_1 - \omega^* / \omega_2 - \omega^*| = |\omega_1 / \omega_2| = |K_1 / K_2|. \quad (2)$$

If the system generating the CM is caused by two coupled oscillators that are driven weakly by the stimulus tone, then from inspection of Figure 9A,  $\omega_1$  and  $\omega_2$  are the two modes of the oscillator at tone onset that have natural frequencies close to 57 and 60.7 kHz. ( $K_1 + K_2$ ) is a constant, and the ratio between the coupling coefficients  $K_1$  and  $K_2$  is determined by the stimulus frequency and the measurement delay of the CM from tone onset, so that for any given measurement  $\omega^* = F_s - \Delta F$ , where  $F_s$  is the stimulus frequency and  $\Delta F$  is the parallel shift of the CM curve with respect to the isofrequency curve at any given measurement delay of CM from tone onset. These relationships are shown as dotted lines in Figure 10A for compromise frequencies  $\omega^* = F_s - 0.2$  kHz and  $\omega^* = F_s - 0.55$  kHz. The coupling strength between the oscillator responsible for the ringing after the tone offset (presumably the TM) and the forced oscillation of the oscillator responsible for the CM responses at the tone onset (presumably the BM) increases with time from tone onset, so that for times longer than 2.3 msec, the CM frequency tends toward the stimulus frequency.

### CM at onset of tones within CRR is compromise frequency dominated by cochlear resonance

Frequencies with the range of the CRR (59.4 and 62.4 kHz) (Figs. 9 and 10) at tone onset excite an oscillator (presumably the TM), which has a single natural frequency close to 60.8 kHz. Within the CRR, CM frequency is proportional to the stimulus frequency. For the data presented in Figure 10A, the slope of the CM frequency–stimulus frequency relationship is 0.337 Hz/Hz. The ratios for this and for four other bats are given in Table 1.

We suggest that within the CRR, the frequencies of the two oscillators, presumably the BM and TM are strongly attracted to each other so they behave as a single oscillator that captures and dominates the OHC responses in the CRR. One of the oscillators (presumably the BM) is also driven by the stimulus tone. Thus, the frequency of the CM in this region is a compromise frequency ( $\omega^*$ ) that is determined by the natural frequency of the single oscillator in the CRR ( $\omega_1$ ), the stimulus frequency ( $\omega_2 = F_s$ ), and

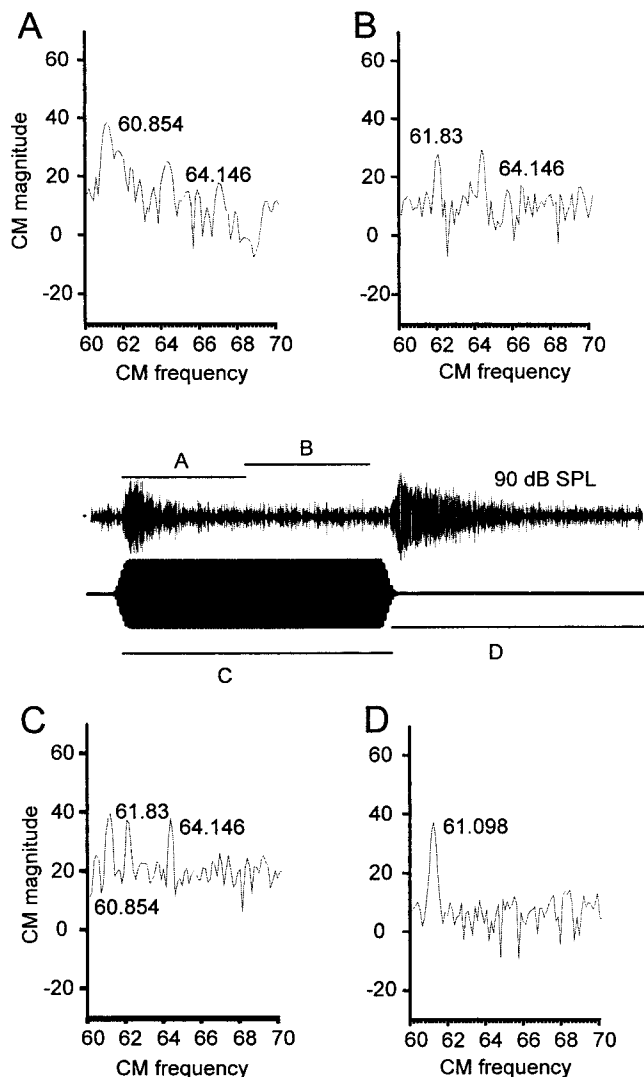


**Figure 8.** Frequency composition of CM changes with time during the on-off response to a 61.83 kHz, 10 msec tone. CM magnitude frequency relationships based on 1024 point FFTs measured 1–5 msec (*A*), 5–11 msec (*B*), 1–11 msec (*C*), and 11–20 msec (*D*) from tone onset.

the relative strengths of the coupling constants ( $K_1$  and  $K_2$ ), as set out in Equation 1. From Figure 10*A*, we can see that  $\omega^* = 60.8$  kHz when  $F_s = 61$  kHz. The slope of the CM frequency–stimulus frequency relationship is 0.337 Hz/Hz in the CRR region, which provides the ratio between  $K_2$  and  $K_1$ . Accordingly, from Equation 1,  $\omega_1 = 60.733$  kHz.

#### CM frequency within cochlear resonance region oscillates about stimulus frequency

If CM is measured with a delay  $>2.3$  msec from tone onset, then for frequencies below and above the CRR, CM is generated by a closely coupled system in that CM frequency equals the stimulus frequency (Fig. 10*B*). If CM frequency is measured within the CRR and within 2 msec of tone onset, then for the data presented in Figures 9 and 10, the CM increases with a slope of 0.337 Hz/Hz with increasing stimulus frequency, i.e., CM frequency is  $\sim 1$  kHz higher than stimulus frequency at the lower boundary of the CRR, and slides down in frequency, relative to the stimulus frequency, with increasing stimulus frequency. CM frequency equals the stimulus frequency at 60.8 kHz and is  $\sim 1$  kHz less than the stimulus frequency at 62.4 kHz (Fig. 10*A*). With increasing

measurement delay from tone onset, the extent of the frequency glide decreases symmetrically about the cochlear resonance frequency (Fig. 10*B*, bottom record). At frequencies within the CRR, but outside the bandwidth of the frequency glide, the CM frequency oscillates about the isofrequency function (Fig. 10*B*, dashed lines), alternating between being greater or smaller than the stimulus frequency. The mean periodicity and the magnitude of frequency excursions of the CM frequency about the isofrequency decrease with increasing measurement delay to values that are limited by the frequency resolution of the analysis technique (125 Hz). For measurement delays between 2.3 and 4 msec, the system responsible for CM generation changes from one in which the frequency changes in proportion to the stimulus frequency to a more closely coupled system that hunts about the desired frequency even 9 msec or more after tone onset (Fig. 10*B*). Within the CRR, the CM does not settle exactly on the stimulus frequency but on a frequency that oscillates a few hundred hertz above or below the stimulus, depending on its frequency.

For frequencies below the CRR and for measurement delays of  $<2$  msec, the CM phase lags at a constant rate with frequency (Fig. 10*C*), presumably because the frequency of the CM is not at the stimulus frequency but at a compromise frequency that is a constant amount below the stimulus frequency. At frequencies above CRR and at a measurement delay  $>2$  msec from the tone onset for frequencies below the CRR, the CM frequency equals, and is in phase with, the stimulus frequency (Fig. 10*D*). Oscillations in the CM frequency in the CRR are associated with phase transitions (Fig. 10). Thus, CM phase measurements made within the CRR, and after a 2 msec delay from tone onset, show considerable jitter that is associated with the frequency hunting behavior.

## Discussion

### CM with and without amplification

CM measurements from the mustached bat's cochlea fovea provide a unique opportunity to compare responses with and without amplification from a cochlea that has not been compromised. The slow build-up of the CM facilitates analysis of the temporal responses of the cochlea to tones at frequencies near the 61 kHz resonance. Within 1 msec of tone onset the CM is that from a passive cochlea without OHC feedback, being relatively insensitive, growing linearly with increasing stimulus level, and broadly tuned. Throughout the ongoing tone and in the ringing after tone offset, the CM is that from a cochlea with active feedback being compressive, sharply tuned ( $Q_{3dB} > 300$ ), and 50–60 dB more sensitive than at tone onset. Thus, in the sharply resonant foveal region of the cochlea, amplification builds up after many cycles of BM vibration at the cochlear resonance frequency. CM magnitudes as functions of tone frequency measured from the “passive” cochlea at tone onset are broader with tips that are a few hundred hertz lower in frequency than those of the active cochlea measured  $>4$  msec from tone onset. In non-echolocating mammals, passive cochlear properties have been measured in preparations that have been compromised through asphyxia, ototoxic drugs, and death itself (for review, see Robles and Ruggero, 2001). In these preparations, the tuning curve peak is shifted, by about half an octave, to lower frequencies. In the mustached bat, the oscillator that dominates the ringing (presumably the TM) and the oscillator that dominates the CM at tone onset (presumably the BM) are tuned to similar frequencies at the transition between the SI region and the more apical CF2 region (Kössl and Vater, 1996). There is a strong indication that in non-echolocating



mammals the TM is tuned to a frequency that is half an octave below that of the BM (Gummer et al., 1996; Legan et al., 2000; Lukashkin and Russell, 2003).

In mechanical models of BM tuning comprising two resonant masses (Allen, 1980; Zwislocki, 1986) (e.g., the BM and the reticular lamina coupled through the OHCs), frequency-dependent amplification occurs if forces generated by OHCs phase lead by 90° passive displacements of the BM (Geisler and Sang, 1995; Markin and Hudspeth, 1995). We find for frequencies of <1 kHz below the cochlear resonance, the amplified and compressive  $CM_{\text{Steady}}$  measured during the ongoing-tone phase leads by 90° the linear, passive  $CM_{\text{ON}}$  measured during tone offset. An indication that OHCs amplify BM vibrations in the foveal region of the mustached bat cochlea by feeding back energy to the cochlear partition during maximum velocity, which is when the forces of TM inertia are synergistic with OHC electromotility (Gummer et al., 1996). A similar conclusion was reached on the basis of BM measurements made in the basal turns of the guinea pig (Nilsen and Russell, 1999) and mouse (Legan et al., 2000) cochleae. For frequencies within 1 kHz below the cochlear resonance, the phase difference between the  $CM_{\text{ON}}$  and  $CM_{\text{Steady}}$  increases to 180°, which corresponds to the region of sharp insensitivity that has been measured in distortion product otoacoustic emissions (DPOAEs), CM, auditory nerve, and BM responses (Fig. 1 of Kössl and Vater, 1996).

### Basis for beating in $CM_{\text{AFT}}$

Beating between the cochlear resonance and stimulus tone (first described by Suga et al., 1977) appears as an amplitude modulation of  $CM_{\text{Steady}}$  that decreases in frequency as the resonance frequency is approached (Figs. 4, 5, and 7). Beating is not usually seen in  $CM_{\text{AFT}}$  because there is nothing for the resonance to beat against. However, in a bat that was anesthetized with isoflurane, the CM was modulated by complex beating between two intrinsic oscillators in the cochlea, which also appeared in  $CM_{\text{AFT}}$ . From their beating periodicity, the natural frequencies of the two components are 61.97 and 62.18 kHz, neither of which is at the 61.5 kHz frequency of the onset oscillator (Fig. 5B). Perhaps anesthesia caused mechanical uncoupling of two components of the cochlear partition so that their natural frequencies, although closely matched, are now expressed separately. Suga et al. (2000) observed beating in  $CM_{\text{AFT}}$  after corticofugal stimulation. The action of isoflurane on smooth muscle (Akata and Boyle, 1995) and the “slow” action of the cochlear efferents on OHCs, which adapts because of desensitization of the acetylcholine receptors that mediate it (Murugasu and Russell, 1996; Sridhar et al., 1997), have both been attributed with causing changes in cellular mechanics through  $Ca^{2+}$  release from ryanodine-sensitive intracellular  $Ca^{2+}$  stores.

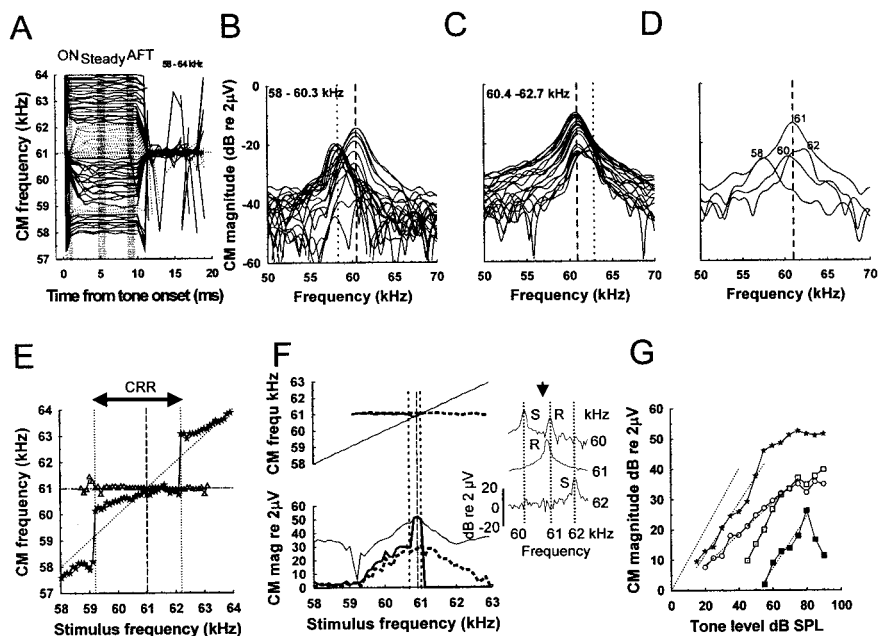


**Figure 9.** *A*, CM frequency recorded from the cochlea of a bat with a cochlear resonance of 61 kHz as a function of time from the onset of 10 msec duration tones with 1 msec rise and fall times stepped in 100 Hz frequency intervals from 58 to 64 kHz at 70 dB SPL. The solid and dotted lines are to guide the eye. *B–D*, FFTs (4096 points, 4  $\mu$ sec interval) applied to the first 0.6 msec of the CM responses to tone burst at frequencies 58–60.3 (*C*) and 60.4–62.7 (*D*) kHz stepped in 0.1 kHz increments. *D*, Selected FFTs from *B* and *C* at 58, 60, 61, and 62 kHz. Vertical dashed line, Resonance frequency; vertical dotted lines in *B* and *C*, secondary resonance frequencies. *E*, CM frequency as a function of stimulus frequency based on the data in *A*. CM measurements were made between 0.6 and 1.6 msec (asterisks) and 0.5 and 1.5 msec after tone offset (triangles). Diagonal dotted line, CM frequency = stimulus frequency; central vertical dashed line, resonance frequency. Data were based on 8192 point FFTs applied to CM data as functions of CM frequency for 1 msec sample periods. *F*, CM frequency (top) and CM magnitude (bottom) measured during the ongoing tone from 2 msec after tone onset to the end of the tone (solid lines) and in the ringing after tone offset (thick dotted lines). The CM is composed of two principal frequency components, a stimulus frequency component (thin line) and a resonance frequency component (thick line). For frequencies below the resonance frequency (vertical dashed line), only the stimulus frequency component is present. Vertical dotted lines indicate the boundaries of the frequencies that attract the resonance. Inset, FFTs (4096 points, 4  $\mu$ sec interval) in response to 60, 61, and 62 kHz tones. Vertical dotted lines indicate positions of stimulus frequency (*S*) and resonance frequency (*R*) components. *G*, CM magnitude as functions of stimulus level measured during the ongoing tone. Dashed line, Slope of 1; dotted lines, regression curves; open squares, stimulus frequency response to 60 kHz tone (regression slope, 1); filled squares, resonance frequency response to 60 kHz tone (regression slope, 0.86); asterisks, stimulus frequency response to 61 kHz (regression slope, 0.85); open circles, stimulus frequency response to 62 kHz (regression slope, 0.52).

### On–off effect attributable to differences in onset and offset oscillators

The on–off transients in  $CM_{\text{Steady}}$ , but not in passive  $CM_{\text{ON}}$  reported here are very similar to those measured in BM mechanics recorded in the basal turn only of sensitive chinchilla cochleae (not postmortem) for frequencies above CF and levels ~90 dB SPL that is associated with a notch and 180° phase shift in the level functions [compare Fig. 11 of Recio and Rhode (2000) with our Fig. 7]. Similar notches and associated phase reversals in response to high-level tones above CF have been observed in OHC receptor-potential level functions (Russell and Kössl, 1992) and were attributed to level-dependent changes in the mechanical coupling of OHC stereocilia to the TM, as first proposed by Zwislocki, 1988.

We suggest that the on–off transients in the  $CM_{\text{Steady}}$  can be accounted for by two oscillators, one broadly (BM) and the other narrowly (TM) tuned to similar frequencies. At tone onset, the responses of the broadly tuned oscillator develop first, whereas the responses of the narrowly tuned oscillator take 2–3 msec longer. At tone offset the broadly tuned oscillator quickly settles, whereas the narrowly tuned oscillator continues to ring. If the two oscillators are in phase, or a factor of a whole cycle apart (Fig. 7B), during the ongoing tone (i.e., 61.9 kHz) (Fig. 6B), then the

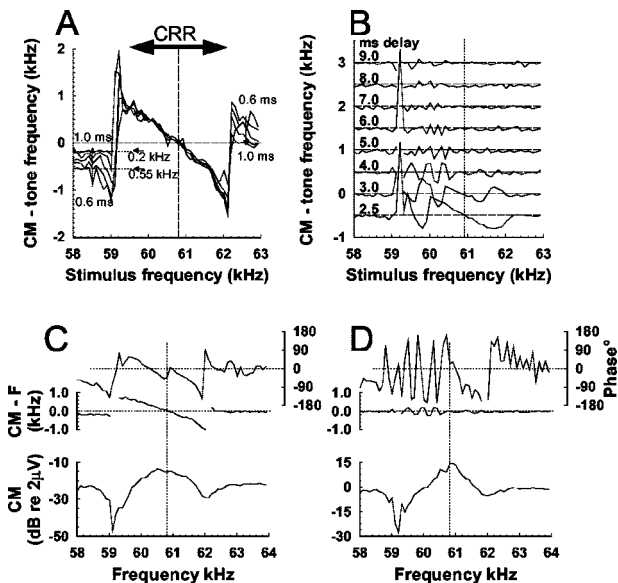


**Figure 10.** *A*, Superimposed curves of the difference between CM frequency and tone as functions of stimulus frequency for CM measurements sampled for 1 msec periods taken with delays from tone onset between 0.6 and 1 msec in increments of 0.1 msec. The vertical dashed line indicates the intersection at 60.8 kHz of the curves and the isofrequency curve (horizontal dashed line). Horizontal dotted lines indicate the compromise frequencies of the CM for frequencies below 59.4 kHz based on Equation 1. Data from the same bat as that shown in Figure 9. *B*, Curves of the difference between CM frequency and tone as functions of stimulus frequency for CM measurements sampled for 1 msec periods taken with delays from tone onset between 2.5, 3, 4, 5, 6, 7, 8, and 9 msec after tone onset. For clarity, each curve is offset by 0.5 kHz. The vertical dotted line indicates the intersection at 60.8 kHz of the curves and the isofrequency curve (horizontal dashed lines). Data from the same bat as that shown in Figure 4*A*. *C*, *D*, CM phase (top trace), frequency (middle trace), and magnitude (bottom trace) as functions of stimulus frequency for measurements made 1 (*C*) and 4.0 (*D*) msec from the onset of 10 msec tone bursts at 75 dB SPL from the cochlear duct of a bat with a cochlear resonance at 61 kHz. Measurements based on 8192 point FFTs applied to CM data.

**Table 1. Slope of CM frequency–stimulus frequency**

Bat ID	$\omega_1$ (kHz)	Slope (Hz/Hz)
Adult	61.248	0.428
Adult2	61.013	0.505
Ppad3	60.733	0.337
Ppic1	62.4	0.365
Ppic7	62.4	0.483

ID, Identity.

net shear displacement between the two oscillators, and the CM magnitude, will be minimal (Zwislocki, 1986).

### Cochlear resonance caused by interaction between two oscillators represented by BM and TM

At frequencies close to the cochlear resonance,  $CM_{ON}$  is not at the stimulus frequency but is at, or close to, one of the frequency modes of the resonance. Within a few milliseconds the CM frequency is at the resonance or hunting about it. Frequency glides reported in impulse responses of auditory nerve and basilar membrane (de Boer and Nuttall, 1997; Carney et al., 1999; Recio and Rhode, 2000) have similar time-dependent frequency behavior that has been attributed to the multiple resonance of each radial cross section of the cochlear partition, and as a consequence of the dispersive properties of wave propagation in the cochlea (Sera, 2001).

We propose that the foveal region of the bat cochlea behaves as a system of coupled, strongly resonant, oscillators. One oscillator (BM) is more broadly tuned to a frequency a few hundred hertz

below that of the more sharply tuned oscillator (TM) (see Figs. 4–8). For frequencies below the CRR, the frequency of the broadly tuned oscillator, which dominates the responses of the CM at tone onset, is a few hundred hertz below the stimulus frequency. This difference decreases with the increasing measurement delay of the CM from tone onset. We suggest that the CM frequency at tone onset is a compromise frequency because of synchronization between the different frequency modes of the onset oscillator and the stimulus tone. The compromise frequency depends on the stimulus frequency, which determines the relative coupling between the oscillators, and on the measurement delay from tone onset. With increasing measurement delay from tone onset, the coupling between the two oscillators changes, presumably because the oscillators are captured and driven by the stimulus frequency.

When the frequency of the CM is not that of the stimulus but a compromise frequency, CM phase will slip and continuously lag behind that of the stimulus according to the frequency difference between the stimulus and CM frequencies (Fig. 10*C*) (frequencies of 58–59 kHz). The CM frequency measured after a delay of 2.5 msec from tone onset is that of the stimulus, and the CM phase over the 58–59 kHz frequency range is independent of stimulus frequency.

### Within CRR, CM dominated by cochlear resonance

At the lower transition frequency of the CRR,  $CM_{ON}$  is strongly attracted by an oscillator with a sharp resonance (TM) that dominates the CM frequency response within the CRR. Notably, the oscillator is actually captured by the stimulus when the frequency is at and above the cochlear resonance. At these frequencies the FFT of the CM is composed of a stimulus frequency and a resonance frequency component, but only a compromise frequency for frequencies below the resonance, which follows the stimulus frequency by a fixed proportion of 0.3–0.5 Hz/Hz. We have proposed a model to fit the data, which, with one exception, is identical to that we have used to fit the responses to frequencies below the CRR (see Eq. 1). The exception is that one oscillator ( $\omega_1$ ) dominates the CRR region and the second oscillator ( $\omega_2$ ) is the BM, which is driven by the stimulus frequency. The relative coupling between the two oscillators is determined by the stimulus frequency.

### CM frequency within CRR oscillates about stimulus frequency

For frequencies within the CRR, the CM frequency measured within the ongoing tone, and >2.3 msec from tone onset, does not change smoothly with increasing stimulus frequency but hunts about it with phase jumps as it overshoots or undershoots it.

This type of synchronization behavior has been observed in other coupled nonlinear biological oscillators (Winfree, 1967; Mirolo and Strogatz, 1990; Strogatz, 1994; Pikovsky et al., 2001). The response to the ongoing tone contains both stimulus frequency and resonance components for frequencies below the resonance frequency. Above the resonance frequency, the resonance component is suppressed by the stimulus frequency, presumably as a consequence of two-tone suppression, which is more effective on the high-frequency side of inner hair cells (Sellsick and Russell, 1979), BM, and neural tuning curves (Ruggero et al., 1992; Cooper, 1996).

$CM_{Steady}$  undergoes a 180° phase transition that is associated with the peak magnitude of the CM (Henson et al., 1985). From BM vibration measurements the resonance and the phase transition have been attributed to a simple oscillator (Kössl and Russell, 1995).  $CM_{AFT}$ , which has a single frequency component at the

cochlear resonance frequency, undergoes a sharp 360° phase transition at the resonance frequency. Thus, the oscillator responsible for the CM<sub>AFT</sub> phase, presumably caused by the interaction between the BM and TM, leads the oscillator responsible for CM<sub>ON</sub> by 180° for frequencies below the cochlear resonance and lags CM<sub>ON</sub> by 180° for frequencies above the resonance. This phase transition is the same as that measured for DPOAEs, in which it has been attributed to the resonance of the TM (Kössl and Vater, 2000). These temporal characteristics of the resonance measured in the CM reinforce the proposal that the cochlear resonance of the mustached bat is caused by OHC-mediated interaction between two oscillators (Russell and Kössl, 1999). The BM in the cochlear fovea behaves as a driven oscillator, which responds to tone-induced pressure differences between the fluid-filled scala vestibule and scala tympani. The TM in the fovea behaves as a coupled oscillator that responds initially to the vibrations of the BM and then dominates the mechanical responses of the cochlear fovea. When the two oscillators are closely matched in frequency, through their interaction via the OHCs, which pump energy cycle-by-cycle into the system (for review, see Robles and Ruggero, 2001), the frequency tuning of the cochlear fovea is exquisite, and highly resonant.

## References

- Akata T, Boyle III WA (1995) Volatile anesthetic actions on contractile proteins in membrane-permeabilized small mesenteric arteries. *Anesthesiology* 82:700–712.
- Allen JB (1980) Cochlear micromechanics: a physical model of transduction. *J Acoust Soc Am* 68:1660–1670.
- Brownell WE, Bader CR, Bertrand D, Ribaupierre YD (1985) Evoked mechanical responses of isolated outer hair cells. *Science* 227:194–196.
- Carney LH, McDuffy MJ, Shekhter I (1999) Frequency glides in the impulse responses of auditory-nerve fibers. *J Acoust Soc Am* 105:2384–2391.
- Cooper NP (1996) Two-tone suppression in cochlear mechanics. *J Acoust Soc Am* 99:3087–3098.
- Dallos P (1985) Response characteristics of mammalian cochlear hair cells. *J Neurosci* 5:1591–1608.
- Dallos P (1992) The active cochlea. *J Neurosci* 12:4575–4585.
- Dallos P, Billone MC, Durrant JD, Wang C, Raynor S (1972) Cochlear inner and outer hair cells: functional differences. *Science* 177:356–358.
- Davis H (1965) A model for transducer action in the cochlea. *Cold Spring Harbor Symp Quant Biol* 30:181–190.
- de Boer E, Nuttall AL (1997) The mechanical waveform of the basilar membrane. I. Frequency modulations (“glides”) in impulse responses and cross-correlation functions. *J Acoust Soc Am* 101:3583–3592.
- Geisler CD, Sang C (1995) A cochlear model using feed-forward outer hair cell forces. *Hear Res* 86:132–146.
- Gummer AW, Hemmert W, Zenner HP (1996) Resonant tectorial membrane motion in the inner ear: its crucial role in frequency tuning. *Proc Natl Acad Sci USA* 93:8727–8732.
- Henson Jr OW, Pollak GD (1972) A technique for chronic implantation of electrodes in the cochleae of bats. *Physiol Behav* 8:1185–1188.
- Henson Jr OW, Schuller G, Vater M (1985) A comparative study of the physiological properties of the inner ear in Doppler shift compensating bats (*Rhinolophus rouxi* and *Pteronotus parnellii*). *J Comp Physiol [A]* 157:587–597.
- Henson Jr OW, Xie DH, Keating AW, Henson MM (1995) The effect of contralateral stimulation on the cochlear resonance and damping in the mustached bat: the role of the medial efferent system. *Hear Res* 86:111–124.
- Kössl M, Russell IJ (1995) Basilar membrane resonance in the mustached bat. *Proc Natl Acad Sci USA* 92:276–279.
- Kössl M, Vater M (1985) The cochlear frequency map of the mustached bat, *Pteronotus parnellii*. *J Comp Physiol [A]* 157:687–697.
- Kössl M, Vater M (1990) Resonance phenomena in the cochlea of the mustache bat and their contribution to the cochlear nucleus of the mustached bat, *Pteronotus parnellii*. *J Comp Physiol [A]* 166:695–709.
- Kössl M, Vater M (1995) Cochlear structure and function in bats. In: *Springer handbook of auditory research. Hearing by bats*, Vol 11 (Popper A, Fay R, eds), pp 191–234. New York: Springer.
- Kössl M, Vater M (1996) Further studies on the mechanics of the cochlear partition in the mustached bat. II. A second cochlear frequency map derived from acoustic distortion products. *Hear Res* 94:78–86.
- Kössl M, Vater M (2000) Consequences of outer hair cell damage for otoacoustic emissions and audio-vocal feedback in the mustached bat. *J Assoc Res Otolaryngol* 1:300–314.
- Legan KP, Lukashkina VA, Goodyear RJ, Kössl M, Russell IJ, Richardson GP (2000) A targeted deletion in  $\alpha$ -tectorin reveals that the tectorial membrane is required for the gain and timing of cochlear feedback. *Neuron* 28:273–285.
- Lukashkin AN, Russell IJ (2003) A second, low frequency mode of vibration in the intact mammalian cochlea. *J Acoust Soc Am* 113:1544–1550.
- Markin VS, Hudspeth AJ (1995) Modelling the active process of the cochlea: phase relations, amplification, and spontaneous oscillation. *Biophys J* 69:138–147.
- Mirollo R, Strogatz S (1990) Synchronization of pulse-coupled biological oscillators. *SIAM J Appl Math* 50:1645–1662.
- Murugasu E, Russell IJ (1996) The role of calcium on the effects of intracochlear acetylcholine perfusion on basilar membrane displacement in the basal turn of the guinea pig cochlea. *Auditory Neurosci* 2:363–376.
- Neuweiler G (1990) Auditory adaptations for prey capture in echolocating bats. *Physiol Rev* 70:615–641.
- Nilsen KE, Russell IJ (1999) Timing of cochlear feedback: spatial and temporal representation of a tone across the basilar membrane. *Nat Neurosci* 2:642–648.
- Patuzzi R, Yates GK, Johnstone BM (1989) The origin of low frequency microphonic in the first turn of guinea pig. *Hear Res* 39:177–188.
- Pikovsky A, Rosenblum M, Kurths J (2001) Synchronization: a universal concept in nonlinear sciences. Cambridge: Cambridge UP.
- Recio A, Rhode WS (2000) Basilar membrane responses to broadband stimuli. *J Acoust Soc Am* 108:2281–2298.
- Robles L, Ruggero MA (2001) Mechanics of the mammalian cochlea. *Physiol Rev* 81:1305–1352.
- Ruggero MA, Robles L, Rich NC (1992) Two-tone suppression in the basilar membrane of the cochlea: mechanical basis of auditory rate suppression. *J Neurophysiol* 68:1087–1099.
- Russell IJ, Kössl M (1992) Modulation of hair cell voltage responses to tones by low-frequency biasing of the basilar membrane in the guinea pig cochlea. *J Neurosci* 12:1587–1601.
- Russell IJ, Kössl M (1999) Micromechanical responses to tones in the auditory fovea of the greater mustached bat's cochlea. *J Neurophysiol* 82:676–686.
- Russell IJ, Sellick PM (1983) Low frequency characteristics of intracellular receptor potentials recorded in mammalian hair cells. *J Physiol (Lond)* 33:179–206.
- Sellick PM, Russell IJ (1979) Two-tone suppression in cochlear hair cells. *Hear Res* 1:227–236.
- Shera CA (2001) Frequency glides in click responses of the basilar membrane and auditory nerve: Their scaling behavior and origin in travelling-wave dispersion. *J Acoust Soc Am* 109:2023–2034.
- Sridhar TS, Brown MC, Sewell WF (1997) Unique postsynaptic signalling at the hair cell efferent synapse permits calcium to evoke changes on two time scales. *J Neurosci* 17:428–437.
- Strogatz SH (1994) Nonlinear dynamics and chaos: with applications to physics, biology, chemistry, and engineering. Reading MA: Addison-Wesley.
- Suga N, Jen PHS (1977) Further studies on the peripheral auditory system of CF-FM bats specialized for fine frequency analysis of Doppler-shifted echoes. *J Exp Biol* 69:207–232.
- Suga N, Simmons JA, Shimoza T (1974) Neurophysiological studies on echolocation systems in awake bats producing CF-FM orientation sounds. *J Exp Biol* 61:379–399.
- Suga N, Simmons JA, Jen PHS (1975) Peripheral specialization for fine analysis of Doppler shifted echoes in the auditory system of the CF-FM bat *Pteronotus parnellii*. *J Exp Biol* 63:61–192.
- Suga N, Gao E, Zhang Y, Ma X, Olsen J (2000) The corticofugal system for hearing: recent progress. *Proc Natl Acad Sci USA* 97:11807–11814.
- von Békésy G (1960) Experiments in hearing. New York: McGraw-Hill.
- Winfree AT (1967) Biological rhythms and the behavior of populations of coupled oscillators. *J Theor Biol* 16:15–42.
- Zwislocki JJ (1986) Analysis of cochlear mechanics. *Hear Res* 22:155–169.
- Zwislocki JJ (1988) Phase reversal of OHC responses at high sound intensities. In: *Cochlear mechanisms: structure and function and models* (Wilson JP, Kemp DT, eds), pp 163–168. London: Plenum.